

Yang-Lee zeros of a random matrix model for QCD at finite density

M.A. Halasz^a, A.D. Jackson^b, and J.J.M. Verbaarschot^a^a Department of Physics, SUNY, Stony Brook, New York 11794^b Niels Bohr Institute, Blegdamsvej 17, Copenhagen, DK-2100, Denmark**Abstract**

We study the Yang-Lee zeros of a random matrix partition function with the global symmetries of the QCD partition function. We consider both zeros in the complex chemical potential plane and in the complex mass plane. In both cases we find that the zeros are located on a curve. In the thermodynamic limit, the zeros appear to merge to form a cut. The shape of this limiting curve can be obtained from a saddle-point analysis of the partition function. An explicit solution for the line of zeros in the complex chemical potential plane at zero mass is given in the form of a transcendental equation.

1. Since the work of Yang and Lee [1], zeros of the partition function have become an important tool for the study of phase transitions. (See, e.g., [2, 3, 4].) Most notably, Yang and Lee proved the theorem that the thermodynamic limit of the free energy is analytic in any region of the complex fugacity plane which contains no zeros. Below, we use the term Yang-Lee zeros as a generic name for zeros of the partition function. (Note, however, that zeros in the complex temperature plane were first discussed in [5, 6].) Historically, Yang-Lee zeros have been studied primarily within the framework of statistical mechanics. Yang-Lee zeros of the Ising model have received particular attention. (See [7] for recent work on this topic.) Recently, however, Yang-Lee zeros were studied in the context of the lattice QCD (QED) partition function for non-zero chemical potential [8, 9, 10, 11, 12]. Because of the difficulty of simulating the partition function of lattice QCD for non-zero chemical potential [13], these studies are still in an exploratory stage. In this work we study Yang-Lee zeros for a much simpler random matrix partition function which possesses the global symmetries of the QCD partition function. This enables us to obtain the Yang-Lee zeros both numerically and analytically.

The continuum Euclidean QCD partition function for a quark mass matrix, m , and chemical potential μ can be written as

$$Z(m, \mu) = \langle \det(\gamma \cdot D + m + i\mu\gamma_0) \rangle_{S_{QCD}}, \quad (1)$$

where $\gamma \cdot D$ is the Euclidean Dirac operator and γ_μ are the Euclidean Dirac matrices. The average is over the Yang-Mills action. In lattice QCD, the chemical potential is incorporated by including a factor e^μ for links forward in time and a factor $e^{-\mu}$ for links backward in time. Since the lattice QCD Dirac operator is a finite matrix, the partition function is a polynomial in m and e^μ . This makes it possible to study zeros of the partition function in the complex fugacity plane. The difficulty with lattice studies is that the coefficients of this polynomial are necessarily obtained numerically. This is problematic because the zeros of a high-order polynomial are notoriously sensitive to the values of its coefficients.

As is well known, the zeros of Z in m are closely related to the chiral order parameter [8]. If these zeros are located at z_k , the partition function (1) can be written as

$$Z(m) = \prod_k (m - z_k). \quad (2)$$

Therefore, the chiral condensate (for one flavor) is given as

$$\Sigma(m) \equiv \frac{1}{N} \partial_m \log Z(m) = \frac{1}{N} \sum_k \frac{1}{m - z_k}. \quad (3)$$

We consider $\Sigma(m)$ as a function of complex m . Provided that these zeros merge to form a cut in the thermodynamic limit, $\Sigma(m)$ will show a discontinuity each time m crosses such a line. Similarly, the ‘baryon density’ defined as $n_B \equiv \partial_\mu \log Z$ shows a discontinuity if μ crosses a line of zeros in the complex μ -plane.

2. In this work we study the Yang-Lee zeros for a random matrix model of the QCD partition function. In essence, we replace the matrix elements of the Dirac operator by Gaussian distributed random variables consistent with the global symmetries of the QCD partition function (see [14] for a review). For N_f flavors this partition function is defined as

$$Z(m, \mu) = \int DCP(C) \prod_f^{N_f} \det \begin{pmatrix} m_f & iC + \mu \\ iC^\dagger + \mu & m_f \end{pmatrix}, \quad (4)$$

where C is an arbitrary complex $n \times n$ matrix and DC the Haar measure. The probability distribution $P(C)$ is given by

$$P(C) = \exp(-n\Sigma^2 \text{Tr}CC^\dagger). \quad (5)$$

We emphasize that this partition function is a *schematic* model of the lattice QCD partition function. For example, it does not reproduce the zero temperature Fermi-Dirac distribution. However, this partition function shares certain important features with the QCD partition function. We mention four properties: 1. This model shows a chiral phase transition as a function of the chemical potential. Chiral symmetry is broken at zero chemical potential and is restored above some critical μ . At $\mu = 0$ the chiral condensate is Σ . 2. The Dirac operator is non-hermitean with eigenvalues distributed in the complex plane. 3. As first shown by Stephanov [15] and confirmed in [16], the quenched limit of this partition function is obtained as the limit $N_f \rightarrow 0$ of (4) with the fermion determinant replaced by its absolute value. 4. If $\mu = i\pi T$, it can be interpreted as a model of the QCD partition function with only the lowest Matsubara frequency included [17, 18, 19]. This model shows a second order phase transition at $\pi T \Sigma = 1$.

Obviously, the partition function (4) is a polynomial in m and μ . The advantage of studying Yang-Lee zeros in this model is that the coefficients of the polynomial can be

obtained analytically. This eliminates a major source of error in the calculation. Here, we restrict our attention to a single flavor, and we adopt units in which the parameter Σ is equal to 1.

Using standard methods [17, 18, 20], this partition function can be rewritten as

$$Z_N(m, \mu) \sim \int d\sigma d\sigma^* e^{-n\sigma\sigma^*} \det^n \begin{pmatrix} \sigma + m & \mu \\ \mu & \sigma^* + m \end{pmatrix}. \quad (6)$$

In the thermodynamic limit this partition function can be evaluated by a saddle point approximation. We obtain a non-trivial saddle point

$$\begin{aligned} \sigma^* &= \sigma, \\ \sigma(m + \sigma)^2 - \mu^2\sigma &= m + \sigma. \end{aligned} \quad (7)$$

For $\mu > 0.527\dots$, the trivial saddle point, $\sigma = 0$, is dominant for $m = 0$ [15]. Chiral symmetry is restored above this point. The point at which the phase change occurs is determined by the solution to a transcendental equation. For complex μ it is given by

$$\text{Re}[\mu^2 + \log(\mu^2)] = -1. \quad (8)$$

We wish to note two special solutions of this equation, $\mu = 0.527\dots$ discussed above and $\mu = i$. The latter solution corresponds to the critical temperature $\pi T = 1$ found in [17]. We will show below that the zeros in μ of $Z(m = 0, \mu)$ for finite n lie along this curve. The discriminant of the cubic equation (7) is given by

$$D_3 = \frac{1}{27}(m^4\mu^2 - m^2(2\mu^4 - 5\mu^2 - \frac{1}{4}) + (1 + \mu^2)^3). \quad (9)$$

We will also show that the endpoints of a line of Yang-Lee zeros are given by the points where this discriminant vanishes.

The partition function (6) can be written as a polynomial in μ and m by a straightforward expansion of the determinant in powers of μ and m . With the help of a number of combinatorial identities, we arrive at

$$Z(m, \mu) = \frac{\pi N!}{N^{N+1}} \sum_{k=0}^N \sum_{j=0}^{N-k} \frac{(Nm^2)^k}{(k!)^2} \frac{(-N\mu^2)^j}{j!} \frac{(N-j)!}{(N-j-k)!}. \quad (10)$$

As a special case we mention $m = 0$, for which the partition function,

$$Z(0, \mu) = \frac{\pi N!}{N^{N+1}} \sum_{j=0}^N \frac{(-N\mu^2)^j}{j!}, \quad (11)$$

is simply a truncated exponential.

3. In this section we evaluate the Yang-Lee zeros of the partition function (10). First, we consider the partition function as a polynomial in m . Fig. 1 shows results for $\mu = 0$, $\mu = 0.5$, and $\mu = 0.6$. We have calculated the zeros for different values of n , e.g., $n = 48$, $n = 96$, and $n = 192$. The results for $n = 192$ are represented by the points in the figure. Of course, the exact location of the zeros is extremely sensitive to numerical round-off errors. Thus, the present results were obtained with the help of a multi-precision package [21]. Typically, we performed our computations with 100-500 digits accuracy.

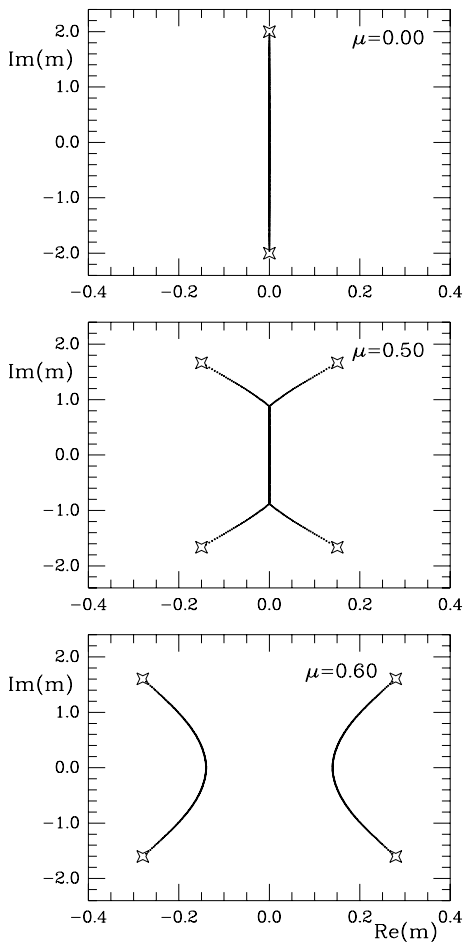


Figure 1: The zeros of the partition function in the complex m plane for $\mu = 0$ (upper), $\mu = 0.50$ (middle) and $\mu = 0.60$ (lower) for $n = 192$. The zeros of the discriminant of the cubic equation (7) are denoted by stars.

The zeros fall on a curve and are regularly spaced¹. From the saddle point analysis of the partition function it is clear that the condition that the free energy of two different

¹If the numerical accuracy is not sufficient, one typically observes that the line of zeros ends in a circle.

saddle point solutions coincides imposes a single condition on the complex variable m . This explains that, in the thermodynamic limit, the zeros are located on a curve in the complex plane (A similar argument has been given for the Ising model [4]). If we increase the order of the polynomial by a factor of 2, we find that half of the zeros are close to those of the lower-order polynomial. The other zeros half are roughly mid-way between adjacent zeros of the lower-order polynomial. This leads us to the conclusion that the zeros become dense and lead to a cut in the complex m plane in the thermodynamic limit.

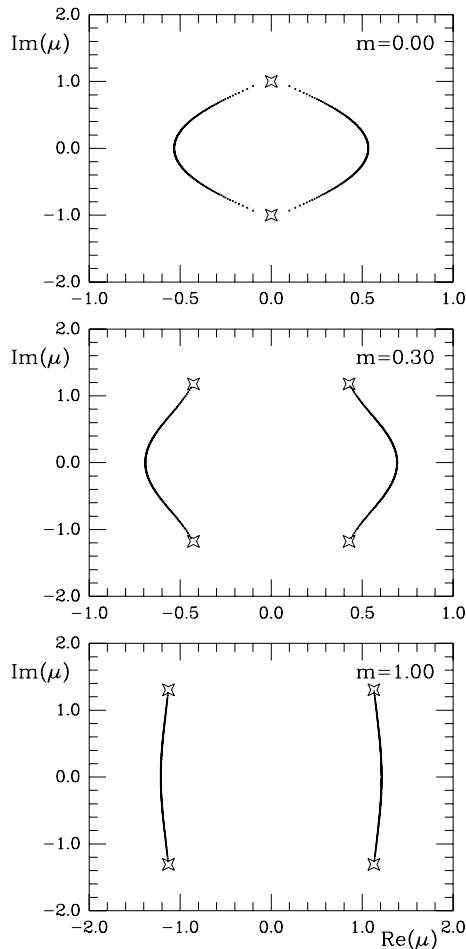


Figure 2: The zeros of the partition function in the complex μ plane for $m = 0$ (upper), $m = 0.30$ (middle), and $m = 1.00$ (lower) for $n = 192$. The solid line in the upper figure represents the solution of the transcendental equation (8). The zeros of the discriminant of the cubic equation (7) are denoted by stars. Note that the scale on the x -axis of the lower figure is different.

The stars in Fig. 1 represent the points at which the discriminant (9) of the cubic saddle point equation vanishes. These points coincide with the endpoints of the line of zeros. We have verified that the line of zeros coincides with the line at which the partition

function is dominated by a different solution of the third-order equation. A schematic picture of this line is shown in [22]. At the critical value of μ , the line of zeros splits into two lines.

In Fig. 2 we show the zeros of the partition function in the complex μ plane for $n=192$ and masses $m = 0$, $m = 0.3$ and $m = 1.0$. We have evaluated the zeros for $n = 48$ and $n = 96$ as well. Also in this case we have performed our calculations with 100-500 digits accuracy. The zeros are regularly spaced and their density increases homogeneously with n . In the thermodynamic limit, we therefore expect that they join into a cut. In all cases the endpoint of the line of zeros ends in a zero of the discriminant (9) (denoted by a star). For $m = 0$ the thermodynamic limit of the line of zeros is given by the solution of the transcendental equation (8) (full line in upper figure). Chiral symmetry is broken in the region enclosed by this curve and is restored outside. Up to corrections of order $1/n$ the zeros coincide with this curve. For $m = 0$ the density of zeros approaches zero near $\mu = i$. This is not surprising since at this point the phase transition changes from first order into second order.

4. In conclusion, we have evaluated the zeros of the partition function in a schematic random matrix model of the chiral transition at non-zero chemical potential. Since the coefficients of these polynomials were obtained analytically, it was possible to locate the zeros numerically with considerable accuracy provided that all arithmetic operations were executed with a precision of 100 to 500 digits. (We stress that calculations with ordinary double or quadruple precision arithmetic are not adequate.) We have found that these zeros lie on one-dimensional subsets in the complex m or μ planes. All of our results are consistent with a mean field analysis of the random matrix partition function. In particular, we have obtained an analytic expression for the curve of zeros in the complex μ plane.

Acknowledgements

This work was partially supported by the US DOE grant DE-FG-88ER40388. We thank Robert Shrock for useful discussions and educating us on to general properties of Yang-Lee zeros. James Osborn is thanked for pointing out the existence of multiprecision packages. Melih Sener is thanked for useful discussions. Finally, we acknowledge D.H. Bailey and NASA Ames for making their multiprecision package available.

References

- [1] C.N. Yang and T.D. Lee, Phys. Rev. **87** (1952) 104; T.D. Lee and C.N. Yang, Phys. Rev. **87** (1952), 410.
- [2] K. Huang, *Statistical Mechanics*, John Wiley and Sons, New York 1987.
- [3] C. Itzykson, R.B. Pearson, and J.B. Zuber, Nucl. Phys. **B220** (1983) 415.
- [4] V. Matteev and R. Shrock, J. Phys. A: Math. Gen. **28** (1995) 5235.
- [5] M.E. Fisher, *Lectures in theoretical physics* vol. 7C, University of Colorado Press, 1965, p. 1.
- [6] S. Katsura, Prog. Theor. Phys. **38** (1967) 1415.
- [7] V. Matteev and R. Shrock, J. Phys. A: Math. Gen. **28** (1995) 1557, 4859; Phys. Rev. E **53** (1996) 254.
- [8] J. Vink, Nucl. Phys. **B323** (1989) 399.
- [9] I.M. Barbour, A.J. Bell, M. Bernaschi, G. Salina, and A. Vladikas, Nucl. Phys. **B386** (1992) 683.
- [10] I.M. Barbour and A.J. Bell, Nucl. Phys. **B372** (1992) 385.
- [11] I.M. Barbour, D.S. Henty, and E.G. Klepfish, Nucl. Phys. **B** (Proc. Suppl.) **34** (1994) 311.
- [12] I.M. Barbour, R. Burioni, G. Di Carlo, and G. Salina Nucl. Phys. **B** (Proc. Suppl.) **34** (1994) 540.
- [13] I. Barbour *et al.*, Nucl. Phys. **B275** (1986) 296; M.P. Lombardo, J. Kogut, and D. Sinclair, hep-lat/9511026.
- [14] J. Verbaarschot, Invited talk at Lattice 96, Nucl. Phys. **B** (Proc. Suppl.) (in press), hep-lat/9607086.
- [15] M. Stephanov, Phys. Rev. Lett. **76** (1996) 4472.
- [16] R.A. Janik, M.A. Nowak, G. Papp and I. Zahed, Phys. Rev. Lett. **77** (1996) 4816.
- [17] A.D. Jackson and J.J.M. Verbaarschot, Phys. Rev. **D53** (1996) 7223.
- [18] T. Wettig, A. Schäfer and H.A. Weidenmüller, Phys. Lett. **B367** (1996) 28.
- [19] A.D. Jackson, M.K. Sener, and J. Verbaarschot, Nucl. Phys. **B** (1996) (in press), hep-th/9602225.
- [20] M. Stephanov, Phys. Lett. **B275** (1996) 249.
- [21] D.H. Bailey, *A Fortran-90 based multiprecision system*, NASA Ames RNR Technical Report RNR-94-013.
- [22] M. Stephanov, Lattice 96, Nucl. Phys. **B** (Proc. Suppl.) (in press), hep-lat/960706.

Figure Captions

Fig.1. The zeros of the partition function in the complex m plane for $\mu = 0$ (upper), $\mu = 0.50$ (middle) and $\mu = 0.60$ (lower) for $n = 192$. The zeros of the discriminant of the cubic equation (7) are denoted by stars.

Fig.2 The zeros of the partition function in the complex μ plane for $m = 0$ (upper), $m = 0.30$ (middle), and $m = 1.0$ (lower) for $n = 192$. The solid line in the upper figure represents the solution of the transcendental equation (8). The zeros of the discriminant of the cubic equation (7) are denoted by stars. Note that the scale on the x -axis of the lower figure is different.